Evaluation and Fabrication of Pore-Size-Tuned Silica Membranes with Tetraethoxydimethyl Disiloxane for Gas Separation

Hye Ryeon Lee, Masakoto Kanezashi, Yoshihiro Shimomura, Tomohisa Yoshioka, and Toshinori Tsuru
Dept. of Chemical Engineering, Hiroshima University, 1-4-1 Kagamiyama, Higashihiroshima 739-8527, Japan

DOI 10.1002/aic.12501
Published online January 19, 2011 in Wiley Online Library (wileyonlinelibrary.com).

Organic/inorganic hybrid silica membranes were prepared from 1,1,3,3-tetraethoxy-1,3-dimethyl disiloxane (TEDMDS) by the sol-gel technique with firing at 300–550°C in N_2. TEDMDS-derived silica membranes showed high H_2 permeance (0.3–1.1 × 10^{-6} mol m^{-2} s^{-1} Pa^{-1}) with low H_2/N_2 (∼10) and high H_2/SF_6 (∼1200) perm-selectivity, confirming successful tuning of micropore sizes larger than TEOS-derived silica membranes. TEDMDS-derived silica membranes prepared at 550°C in N_2 increased gas permeances as well as pore sizes after air exposure at 450°C. TEDMDS had an advantage in tuning pore size by the "template" and "spacer" techniques, due to the pyrolysis of methyl groups in air and Si—O—Si bonding, respectively. For pore size evaluation of microporous membranes, normalized Knudsen-based permeance, which was proposed based on the gas translation model and verified with permeance of zeolite membranes, reveals that pore sizes of TEDMDS membranes were successfully tuned in the range of 0.6–1.0 nm. © 2011 American Institute of Chemical Engineers *AIChE J,* 57: 2755–2765, 2011

Keywords: silica membranes, 1,1,3,3-tetraethoxy-1,3-dimethyl disiloxane (TEDMDS), pore size tuning, micropore

Introduction

Amorphous silica membranes can be used in various types of separation applications because of their chemical and physical stability and low energy consumption. Silica membranes derived by chemical vapor deposition (CVD) and the sol-gel method have been studied most extensively for gas separation.[1,2] In general, tetraethylorthosilicate (TEOS) has been used as the silica precursor for the fabrication of silica membranes. The CVD process generally provides denser structures, resulting in lower permeance and higher selectivity for hydrogen,[3–6] while the sol-gel process usually produces more open structures that offer higher permeance but relatively lower selectivity.[7,8] Silica membranes prepared with TEOS consist of amorphous silica networks with micropores of ∼0.3 nm that allow small molecules such as helium and hydrogen, to permeate. The pore size is appropriate for the separation of hydrogen from small molecules such as N_2 (kinetic diameter: 0.36 nm) and CO_2 (0.33 nm), but appears to be too small for separation of the mixtures with large molecules such as n-C_4H_{10} (0.43 nm) and i-C_4H_{10} (0.50 nm). The design and control of membranes is, therefore, quite important.

Pore size control of microporous silica membranes was first proposed by Raman and Brinker[9] in 1995 as the "template" technique. Silica sols derived from structured-alkoxides that have organic ligands such as methyl and phenyl were coated and fired in an N_2 atmosphere to a covert organic/inorganic mixed matrix, followed by firing in air. Organic ligands that are burned out in air, making pore spaces, can be used as a "template" to control pore size and porosity. Structured alkoxides used with this method include methyltriethoxysilane (MTES)[10–12] and other alkyltriethoxysilanes such as

Correspondence concerning this article should be addressed to T. Tsuru at tsuru@hiroshima-u.ac.jp

octyltriethoxysilane (C8TES), dodecyltriethoxysilane (C12TES), octadecyltriethoxysilane (C18TES),[13] and methacryloxypropyltrimethoxysilane (MOTMS).[14] Several research groups have also reported on possible pore size control with the CVD method, using structured alkoxides consisting of a single silicon atom with phenyl[15–18] or alkyl functional groups (methyl and propyl).[18]

Our group recently proposed another strategy to control the pore size of silica membranes using a bridged alkoxide, which is one of the structured alkoxides and consists of organic functional groups between two silicon atoms. This is called the "spacer" technique. The design of silica networks was reported previously using bis(triethoxysilyl) ethane (BTESE, Si—C—C—Si unit structure) as a silica precursor in the development of a highly permeable hydrogen separation membranes with hydrothermal stability.[19,20] BTESE-derived silica membrane showed extremely high H_2 permeance (as high as 10^{-5} mol m^{-2} s^{-1} Pa^{-1}) with separation factors moderate for H_2/N_2 (~20), and quite high for H_2/SF_6 (~20,000), showing higher permeance and a lower H_2/N_2 permeance ratio than pure SiO_2 membranes. Gas permeation results suggested that BTESE-derived silica membranes had a looser structure than silica membranes prepared with single Si atom unit precursors such as TEOS. The average pore size was estimated to be ~0.5 nm and 0.3 nm, respectively, based on qualitative evaluation of permeance dependence on the kinetic diameter of permeation gases. The membrane with moderate H_2/N_2 and high H_2/SF_6 perm-selectivity which corresponds to relatively large pore size ~0.5 nm could be used for separation of mixtures in many industrial applications, including CO_2/CH_4, H_2/organic gases and organic/organic gas mixtures such as propylene/propane.

Generally, for the estimation of pore size distribution less than 1 nm, the permeances of several gases with different molecular sizes were measured at high temperatures to reduce the effect of surface flow, and the pore sizes were determined only qualitatively, based on permeance ratios such as He/N_2 and He/SF_6, since no theoretical model is available for the determination of subnano-meter pore sizes. The determination of pore sizes is very important for the preparation, characterization and application of porous membranes, and it is crucial to evaluate and choose appropriate alkoxides for specific separation systems. The bubble-point method and bubble-point with gas permeation method allow the measurement of pore sizes larger than 50 nm, while pore sizes in the range of 0.5–30 nm, or more practically 1–20 nm, can be measured by NanoPermporometry.[21] Duke et al. reported the use of positron annihilation lifetime spectroscopy for measurement of subnanometer pores using amorphous molecular sieving silica bulks.[22] However, positron annihilation lifetime spectroscopy is a quite new technique, and is not yet commonly available. Although N_2 adsorption method could be used for measurement of pore size, it is difficult to measure less than 3.64 Å (molecule size of N_2).

In the present study, we propose the normalized Knudsen-based permeance for the determination of membrane pore sizes less than 1 nm, which is based on the gas translation model originally proposed by Xiao and Wei[23] and Shelkhin et al.[24] Based on the contribution of Knudsen diffusion to experimental permeance, pore size can be quantitatively determined. The proposed model was verified with the permeance of zeolite membranes such as MFI and DDR, which were reported to have intrinsic pores 0.55 × 0.56 nm and 0.36 × 0.44 nm, respectively. Moreover, 1,1,3,3-tetraethoxy-1,3-dimethyl disiloxane (TEDMDS) with Si—O—Si bonding (thermally stable) as a "spacer" as shown in Figure 1, was selected to control the loose silica networks. Since TEDMDS has organic ligands (methyl-group) as shown in molecular structure (Figure 1), TEDMDS is a promising alkoxide, the pore size of which could be tuned by both "template (methyl group)" and "spacer (—Si—O—Si— bonding)" technique, depending on firing gas atmosphere during the calcinations. Single gas permeation properties and the thermal stability of TEDMDS-derived silica membranes prepared by the sol-gel method were evaluated. The pore size for TEDMDS-derived silica membranes prepared at various temperatures in a nitrogen atmosphere was estimated using the proposed model.

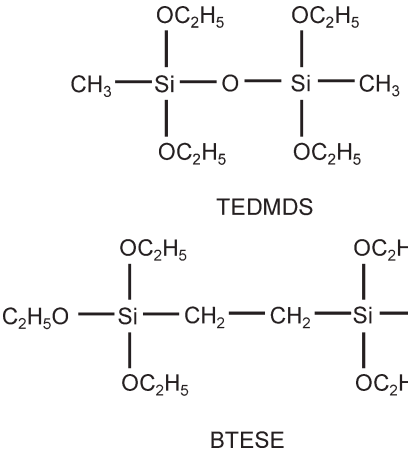

Figure 1. Structures of tetraethoxydimethyl disiloxane (TEDMDS) and bis (triethoxysilyl) ethane (BTESE).

Proposal of normalized Knudsen-based permeance for pore-size determination

Permeation mechanisms of gases through porous membranes can be categorized as viscous flow (molecular diffusion), Knudsen, surface diffusion, and molecular sieving, depending on the structures (molecular size and shape, pore size), the interaction between permeating molecules and membrane pore walls, and operating conditions (pressure, temperature). In viscous flow, permeating molecules collide with one another more frequently than with the wall, resulting in the absence of separation properties for mixed gases. On the other hand, permeating molecules collide with pore walls more frequently than with one another in Knudsen diffusion, resulting in separation ability based on Knudsen diffusivity. In the Knudsen mechanism, the permeance, P_K, through a membrane (pore radius, d_p; membrane porosity, ε; tortuosity, τ; thickness, L) is formulated as follows, using the molecular weight of the permeating component, M, and the temperature, T.

$$P_{K,i} = \varepsilon \frac{d_p}{3} \sqrt{\frac{8RT}{\pi M_i}} \frac{1}{RT\tau L} \tag{1}$$

Surface diffusion occurs for molecules having a large interaction with pore surfaces, but this plays a minor role at

high temperatures due to a decreased amount of adsorption. The following permeation equation, which is referred to as the gas-translation model (GT model) or activated Knudsen, was derived for diffusion through microporous inorganic membranes, using probability, ρ, which indicates the probability of diffusion through the micropore.[23–26]

$$P_i = \varepsilon_i d_{\mathrm{p},i} \rho_i \sqrt{\frac{8RT}{\pi M_i}} \frac{1}{RT \tau_i L_i} \tag{2}$$

Membrane structural factors (pore size, porosity, tortuosity, thickness) are expressed as $d_{\mathrm{p},i}$, ε_i, τ_i, and L_i, due to possible dependence on molecular sizes. Since the probability, ρ, is expressed in Eq. 3 with the pre-exponential, ρ_{g}, and the kinetic energy, E_{p}, to overcome the diffusion barrier, the permeance in Eq. 2 can be expressed in Eq. 4.

$$\rho_i = \rho_{\mathrm{g},i} \exp\left(-\frac{E_{\mathrm{p},i}}{RT}\right) \tag{3}$$

$$P_i = \varepsilon_i d_{\mathrm{p},i} \rho_{\mathrm{g},i} \sqrt{\frac{8RT}{\pi M_i}} \frac{1}{RT \tau_i L_i} \exp\left(-\frac{E_{\mathrm{p},i}}{RT}\right) \tag{4}$$

$\rho_{\mathrm{g},i}$, which is the probability of the i-th component at an infinite kinetic energy, corresponds to the geometrical probability, that is, effective area for permeation, and can be defined by the following equation.

$$\rho_{\mathrm{g},i} = \frac{1}{3} \frac{A_i}{A_0} \tag{5}$$

where A_i is the area of the pore opening for effective permeation of the i-th component, and A_0 is the cross-sectional area of the pore. The fraction 1/3 indicates the one-dimensional direction through the membrane pore. According to GT model, Eq. 4 covers the activated diffusion ($E_{\mathrm{p}} > 0$), surface diffusion ($E_{\mathrm{p}} < 0$) and Knudsen diffusion ($E_{\mathrm{p}} = 0$). The activation energy can be determined by the interactions between permeating molecules and the pore wall, based on the Lennard-Jones potential using the size (membrane pore size, molecular size of permeating molecules) and the interaction parameters.[24]

Herein, we propose the following normalized Knudsen-based permeance, f, that is, the permeance ratio of the i-th component (P_i), to that predicted from j-th component based on Knudsen diffusion mechanism $\left(P_j \sqrt{\frac{M_j}{M_i}}\right)$.

$$f = \frac{P_i}{P_{\mathrm{He}} \sqrt{M_{\mathrm{He}}/M_i}} \tag{6}$$

When He, the smallest molecule, is taken as a reference (j-th component), $P_{\mathrm{He}} \sqrt{M_{\mathrm{He}}/M_i}$ is the permeance of the i-th component predicted from He permeance under the Knudsen diffusion mechanism, and therefore, f corresponds to the ratio of experimentally obtained permeance to predicted permeance based on He. It should be noted that f equals one for the Knudsen mechanism, and f indicates how much the experimentally obtained permeance is decreased due to the molecular sieving effect.

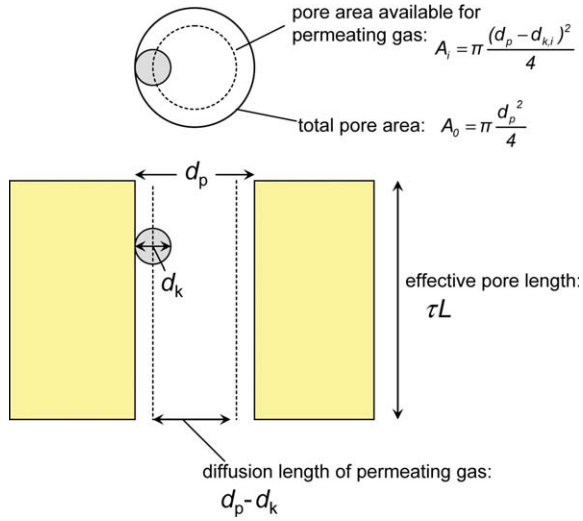

Figure 2. A schematic of micropore permeation of a molecule of molecular size d_k through a cylindrical pore (pore size: d_p).

[Color figure can be viewed in the online issue, which is available at wileyonlinelibrary.com.]

As schematically shown in Figure 2, following Xiao and Wei,[23] the diffusion distance $d_{\mathrm{p},i}$ in Eqs. 2 and 4 is assumed to be $(d_{\mathrm{p}} - d_{\mathrm{k},i})$ for the i-th component (molecular size: $d_{\mathrm{k},i}$), since the center of the i-th component cannot approach the wall. The present model considers the sizes of permeation molecules, while in the original GT model as well as Knudsen, the molecular size is not explicitly incorporated. Moreover, the i-th component can access a pore area with a diameter of $(d_{\mathrm{p}} - d_{\mathrm{k},i})$. Therefore, A_i, the area of the pore opening effective for diffusion, is proportional to the effective pore area.

$$\rho_{\mathrm{g}} = \frac{1}{3} \frac{A_i}{A_0} = \frac{1}{3} \frac{(d_{\mathrm{p}} - d_{\mathrm{k},i})^2}{d_{\mathrm{p}}^2} = \frac{1}{3} \left(1 - \frac{d_{\mathrm{k},i}}{d_{\mathrm{p}}}\right)^2 \tag{7}$$

Based on the above discussion, which is quite similar to the derivation of Ferry's equation commonly used and accepted for the analysis of solute permeation in ultrafiltration, the following expression for normalized Knudsen-based permeance can be obtained by combining Eqs. 4, 5, and 7.

$$f = \frac{P_i}{P_{\mathrm{He}}} \frac{\sqrt{M_i}}{\sqrt{M_{\mathrm{He}}}} = \frac{d_{\mathrm{p},i} \rho_{\mathrm{g},i} \frac{\varepsilon_i}{\tau_i L_i}}{d_{\mathrm{p,He}} \rho_{\mathrm{g,He}} \frac{\varepsilon_{\mathrm{He}}}{\tau_{\mathrm{He}} L_{\mathrm{He}}}} \cdot \exp\left(-\frac{E_{\mathrm{P},i} - E_{\mathrm{P,He}}}{RT}\right)$$
$$= \frac{\left(1 - d_{\mathrm{k},i}/d_{\mathrm{p}}\right)^3}{\left(1 - d_{\mathrm{k,He}}/d_{\mathrm{p}}\right)^3} \exp\left(-\frac{E_{\mathrm{P},i} - E_{\mathrm{P,He}}}{RT}\right) \tag{8}$$

Equation 8 indicates that f can be expressed with the configurational factors (pore size d_{p}, molecular size $d_{\mathrm{k},i}$) and the activation energies of the permeances of He and the i-th component, which need a set of experimental data on the temperature dependence of permeances. In the present study, for simplicity, the assumption has been made that the activation energies, $E_{\mathrm{p},i}$, are the same for any type of gas, to propose a convenient and easy-to-use measurement to evaluate

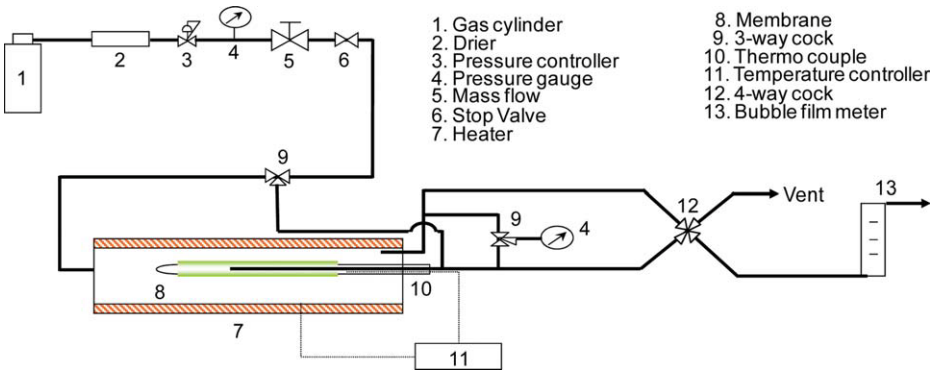

Figure 3. A schematic diagram of the gas permeation apparatus.

[Color figure can be viewed in the online issue, which is available at wileyonlinelibrary.com.]

the pore sizes of microporous membranes. It should be noted that the present model is intended to characterize pores of relatively large size (from several to 10 Å), leading to activation energies which are relatively small or zero (Knudsen diffusion), as was the case for BTESE-derived membranes.[20] Moreover, membrane structural factors such as tortuosity, τ_i, and membrane thickness, L_i, are rationally assumed to be the same irrespective of the molecules, due to a cylindrical pore structure, leading to the following expression for f.

$$f = \frac{\left(1 - d_{k,i}/d_p\right)^3}{\left(1 - d_{k,He}/d_p\right)^3} \tag{9}$$

The procedure to obtain the pore sizes, d_p, of microporous membranes is as follows. First, experimentally obtained permeances are plotted after conversion to normalized Knudsen-based permeance, f ($=\frac{P_i}{P_{He}}\frac{\sqrt{M_i}}{\sqrt{M_{He}}}$), as a function of molecular size, and are then best-fitted with Eq. 9, using d_p as a fitting parameter.

Experimental

Preparation of TEDMDS-derived silica membrane

TEDMDS-derived silica sol was synthesized by hydrolysis and polymerization of TEDMDS, according to previously published methods.[27] The specified amounts of TEDMDS and water in ethanol, with CH_3COOH as an acid catalyst, and were stirred at 60°C for 24 h. The composition of the solution was TEDMDS: H_2O: CH_3COOH = 1: 40: 0.2 in a molar ratio.

A porous α-alumina tube (NOK, Japan, O.D. = 3.0 mm, pore size = 100–150 nm) was used as a support for the TEDMDS-derived silica membrane. An intermediate layer was formed with SiO_2-ZrO_2 (Si/Zr = 1) sol solutions by hot coating followed by firing at 550°C. After formation of an intermediate layer, the TEDMDS-derived silica membrane was fabricated by coating 0.5 wt % of TEDMDS sol at 180°C, followed by firing between 300 and 550°C in an N_2 atmosphere. The morphology of TEDMDS-derived membrane was observed using a scanning electron microscope energy dispersive spectroscopy (SEM-EDS, JCM-5700, JEOL, Japan).

Characteristics of TEDMDS Gel

The decomposition behavior of the organic components was measured by thermogravimetric mass spectrometer (TGA-DTA-PIMS 410/S, Rigaku, Japan). TEDMDS-derived gel powder was prepared by drying at 40°C in air and ground using a mortar. TG-MASS analysis was conducted on the TEDMDS-derived powder, to evaluate the decomposition behavior of organic components with a ramping rate of 20°C·min^{-1} up to 1000°C with 300 ml min^{-1} of He and He/O_2 (=4/1). The TEDMDS-derived film coated on the KBr plate was fired between 300 and 550°C in an N_2 and air atmosphere, and characterized by Fourier transform infrared (FTIR) spectroscopy (FTIR-8300, Shimadzu, Japan).

Single gas permeation measurement and thermal stability test

Figure 3 shows a schematic diagram of gas permeation equipment. Before measurement, the membranes were pretreated to remove the adsorbed water with helium flow at 250–300°C overnight. A single gas (He, H_2, N_2, or C_3H_8) was fed to the outer surface of the membrane at fixed pressure at 150–200 kPa, keeping the permeate stream at atmospheric pressure. SF_6 was fed to the gas permeation equipment at 600 kPa. The temperature of the permeation cell was kept at 50–550°C. The permeation rate was measured by a bubble film meter. For *in situ* heat treatment in air for a membrane, the temperature in the membrane cell was increased at a ramping rate of 2°C·min^{-1} up to 300, 450, and 550°C in air atmosphere. The time courses of air permeance were measured at 300, 450, and 550°C to confirm the steady-state.

Result and Discussions

Verification of normalized Knudsen-based permeance by various porous membranes

Figures 4a,b shows permeances, reported for MFI[28] and DDR[29] membranes, as a function of kinetic diameters. A permeation temperature of 200°C was chosen to reduce the contribution of surface diffusion, since the present model is based on the GT model. The dotted curves show predicted permeance, $P_{He}\sqrt{M_{He}/M_i}$, which is based on He permeance under the Knudsen diffusion mechanism, since He is the

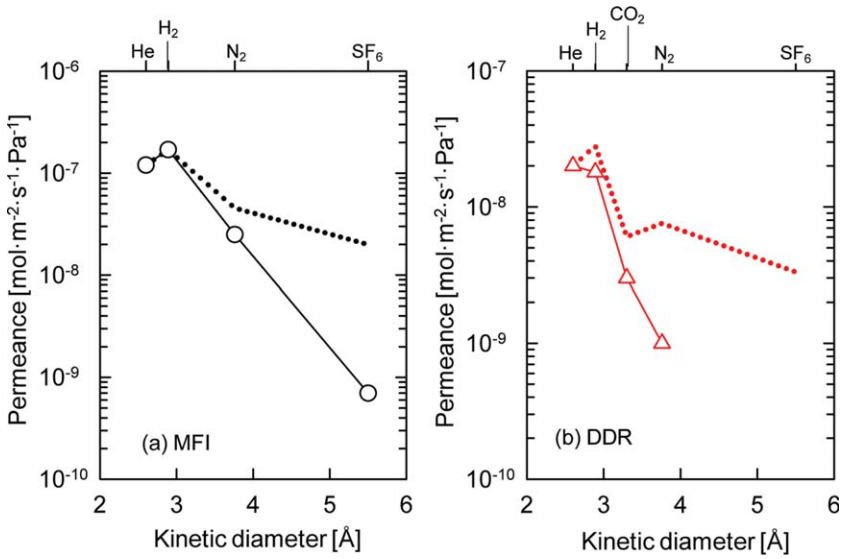

Figure 4. Gas permeance at 200°C as a function of kinetic diameters: points are experimental; dotted line shows predicted permeance using $P_i = P_{He}\sqrt{M_i/M_{He}}$; (a) MFI membrane[28] and (b) DDR membrane.[29]

[Color figure can be viewed in the online issue, which is available at wileyonlinelibrary.com.]

smallest molecule with no adsorption properties. The experimentally obtained permeances agreed well with the predicted ones for small molecules such as H_2, and deviated for larger molecules due to the molecular sieving effect. SF_6 showed 10^1–10^3 times smaller permeance than the Knudsen-based prediction. The ratio of experimentally obtained permeance to Knudsen-based predicted permeance, f, indicates the degree of permeance reduction due to molecular sieving.

Figures 5a,b shows normalized Knudsen-based permeance as a function of molecular size, for MFI[28,30,31] and DDR[29,32,33] membranes, respectively. MFI and DDR membranes are reported to have pores of 0.55 × 0.56 nm and 0.36 × 0.44 nm, respectively. By assuming $d_p = 0.55$ for MFI membranes, normalized Knudsen-based permeances experimentally obtained at 200°C were predicted well by a curve calculated by Eq. 9. Normalized Knudsen-based permeances for DDR membranes were calculated for $d_p = 0.36$ and 0.44 nm and are shown with solid and dotted curves, respectively. Van den Bergh et al.[33] measured the permeances of He, H_2 and N_2 in the range of 30–600°C, while the CO_2 and CO permeances through DDR membrane were measured up to 400°C. Normalized Knudsen-based permeance for CO_2 and CO decreased from 4.97 to 0.72 and from 0.66 to 0.19, respectively, with an increase in permeation temperatures from 100 to 400°C. As shown in Eq. 8, normalized Knudsen-based permeance consists of configurational factors (temperature-independent) and the interaction between permeating molecules and the membrane (expressed as the activation energy, temperature-dependent). CO_2, which is an adsorptive gas, showed larger normalized Knudsen-based permeance than the calculated values even at 400°C, probably due to the contribution of surface diffusion

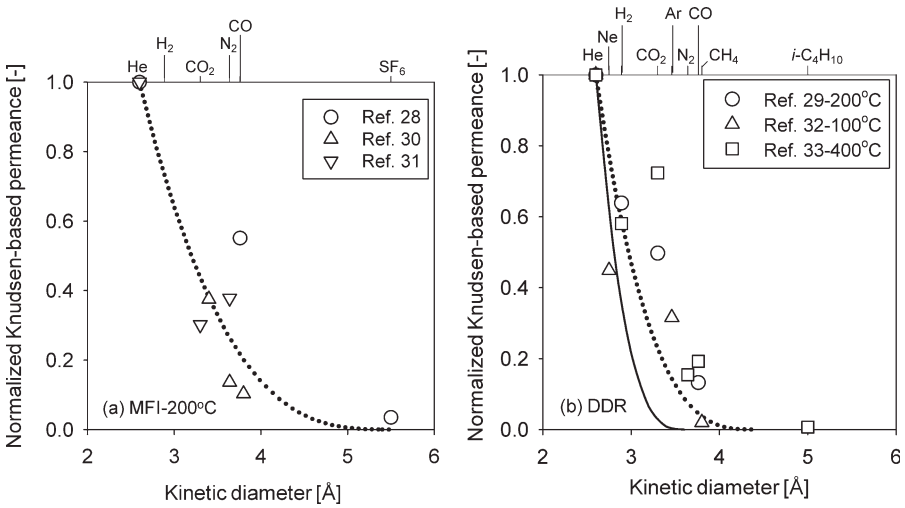

Figure 5. Normalized Knudsen-based permeance as a function of molecular size; points are experimental, and curves are calculated based on Eq. 9 using 0.55 nm for MFI (a), and 0.36 and 0.44 nm for DDR (b).

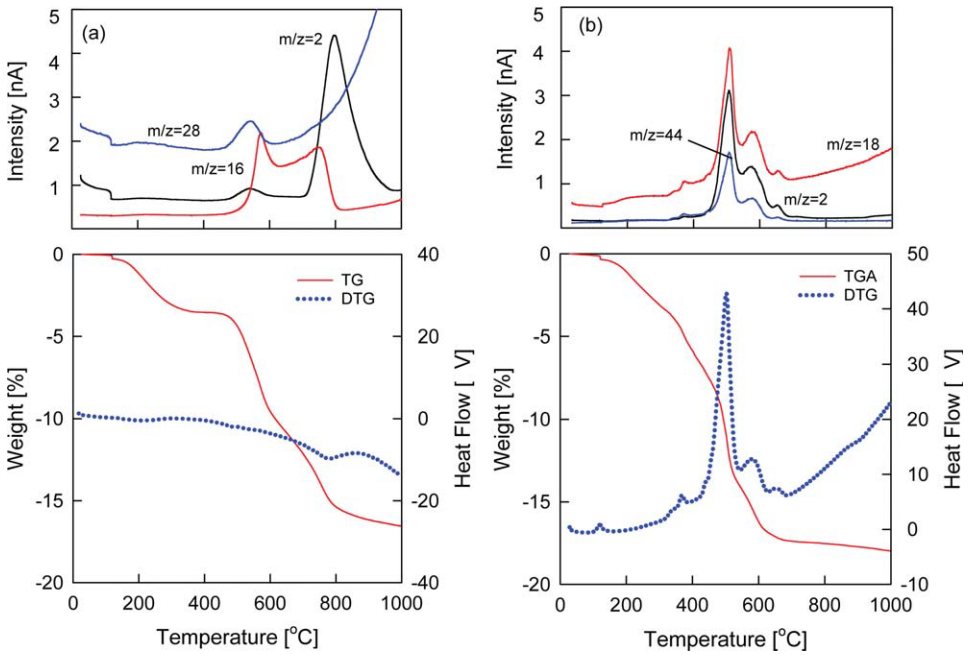

Figure 6. TGA-DTG-MASS curve of TEDMDS-derived silica gel powder in a He and a He/O_2 (=4/1) atmosphere as a function of temperature; (a) He atmosphere, (b) He/O_2 atmosphere.

[Color figure can be viewed in the online issue, which is available at wileyonlinelibrary.com.]

and/ or large interaction with the membrane. Since the exponential term in Eq. 8 approaches to unity and the contribution of surface diffusion decreases at high temperatures, permeation experiments at high temperatures are preferable to obtain pore size based on Eq. 9. As a whole, the calculated curve for $d_p = 0.44$ nm showed good agreement with experimental data measured at higher temperatures.

The proposed technique, "normalized Knudsen-based permeance," which is derived from the GT permeation model with clear assumptions, offers a convenient and easy-to-use measurement to evaluate the pore sizes of microporous membranes.

Characteristics of TEDMDS-derived silica gel

Figures 6a,b show the intensity of mass signals and TGA/DTG curve of TEDMDS-derived silica gel powder under He and He/O_2 atmosphere as a function of temperature, respectively. TEDMDS-derived silica gel powder in He atmosphere showed only a slight weight loss up to 100°C, and residual weight showed a decrease from 100 to 300°C and a drastic decrease from 450 to 850°C in Figure 6a. The weight loss of TEDMDS-derived gel powder up to 300°C was 3.1%, and this can be explained by the evaporation of adsorbed water, ethanol solvent, acetic acid catalyst and/ or decomposition of unreacted ethoxy groups in TEDMDS. On the other hand, the weight loss from 450 to 850°C was 12.9%, probably due to decomposition of unreacted ethoxy groups and/ or methyl groups in TEDMDS polymer. The detection curve of mass number 28 and 16, which can be attributed to C_2H_4, C_2H_6, and CH_4 from the decomposition of unreacted ethoxy groups and methyl groups, appeared around 450°C, respectively. A high peak for m/z = 16 appeared at 550°C, due to the decomposition of methyl groups. The detection curve of CH_4 (m/z = 16) and H_2 (m/z = 2), which appeared at temperatures higher than 700°C, can be explained as the loss of methyl groups, as at high temperatures, methyl groups (≡Si—CH_3) were reported to form ≡Si—C—Si≡ and release H_2, CH_4, and C_2H_4.[34]

On the other hand, Figure 6b shows the intensity of mass signals and TGA/DTG curve in He/O_2 atmosphere as a function of temperature. TEDMDS-derived powder under He/O_2 atmosphere showed exothermic reaction from DTG curve at

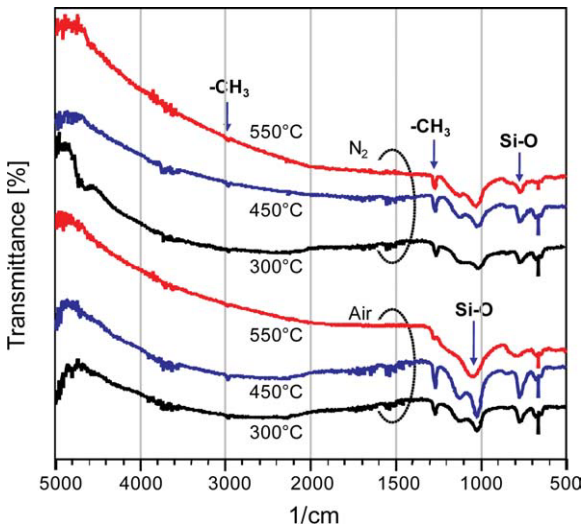

Figure 7. FTIR spectra of TEDMDS-derived silica on the KBr plate fired at different temperatures in a N_2 and an air atmospheres.

[Color figure can be viewed in the online issue, which is available at wileyonlinelibrary.com.]

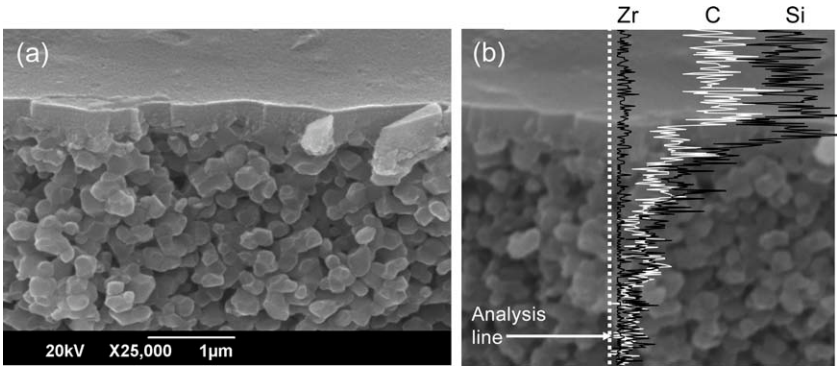

Figure 8. SEM and SEM-EDS images of TEDMDS-derived silica membrane on an α–alumina tube; (a) SEM image, (b) EDS signal of Si, C, and Zr by line analysis.

lower part of Figure 6b. It could be due to combustion of carbon compounds such as unreacted ethoxy or methyl groups in TEDMDS polymer. The detection curves of H_2O and CO_2 from the combustion of carbon compound groups, appeared around 350, 500, and 600°C as mass numbers 18 and 44, respectively. Especially, the detection curves of H_2O and CO_2 showed high intensity around 500°C with drastic weight loss due to the combustion of methyl groups in TEDMDS-derived gel powder under He/O_2 atmosphere. The detection curve of H_2 ($m/z = 2$), which appeared at the same temperatures as $m/z = 18$ and $m/z = 44$, can be explained as a part of methyl groups released H_2 even though He/O_2 atmosphere. If methyl groups were completely decomposed in TEDMDS-derived powder, in theory the weight loss could be 22.4%. However, the total weight losses of the TEDMDS-derived silica powder were 16.5 and 18.0% at He and He/O_2 atmosphere, respectively. It suggests that a few of CH_3 groups were remained in TEDMDS-derived silica powder under He and He/O_2 atmosphere.

Figure 7 shows the FTIR transmission spectra in the range of 500–5000 cm^{-1} for TEDMDS-derived films, which were coated on the KBr plate and fired at 300, 450, and 550°C in air and N_2. The two peaks of Si—O bonding were assigned as follows: the main high frequency band at about 1070 cm^{-1} was due to the asymmetric stretching of the oxygen atoms; the band at frequency near 800 cm^{-1} is ascribed to the symmetric stretching of oxygen atoms.[35] The bands at 1260 and 2900–3000 cm^{-1} were ascribed to the Si—CH_3 bands,[35] suggesting the methyl groups still existed in the film fired at 550°C in a nitrogen atmosphere. However, 1260 cm^{-1} from the Si—CH_3 band almost disappeared at 550°C in air, suggesting combustion of methyl groups might start between 450 and 550°C. FTIR result coincided with the result of TGA-DTG-MASS in Figure 6.

Gas permeation characteristics of TEDMDS-derived membrane

Figures 8a,b show a SEM and SEM-EDS images of the TEDMDS-derived silica membrane prepared at 450°C in an N_2 atmosphere. A crack-free silica layer was successfully formed on a SiO_2—ZrO_2 intermediate layer in Figure 8a, although the boundary was not clearly observed. The intermediate layer combined with the separation layer was approximately 400–500 nm thick on the porous α–alumina layer, which consisted of α–alumina particles 200–300 nm in size. EDS line analysis in Figure 8b suggested that the separation layer consisting of Si and C element was approximately 100–200 nm in thickness based on the intensity of C component.

Figure 9 shows the gas permeance at 200°C for TEDMDS-derived silica membranes (M-1, M-2, and M-3), a TEOS-derived silica membrane,[8] and a BTESE-derived silica membrane[20] as a function of gas kinetic diameter. The BTESE-derived membrane showed a high hydrogen permeance of 1×10^{-5} mol m^{-2} s^{-1} Pa^{-1} with a high H_2/SF_6 perm-selectivity of 1000 and a low H_2/N_2 perm-selectivity (~10). TEDMDS-derived silica membranes were prepared at 300°C (M-1), 450°C (M-2), and 550°C (M-3) in an N_2 atmosphere. All gas permeances for TEDMDS-derived silica membrane increased as the firing temperature increased.

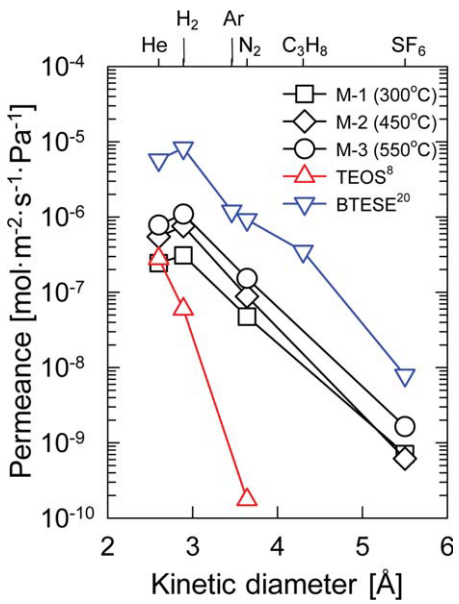

Figure 9. Gas permeance of TEDMDS (M-1, M-2, M-3), TEOS,[8] and BTESE[20]-derived silica membrane at 200°C as a function of kinetic diameter.

[Color figure can be viewed in the online issue, which is available at wileyonlinelibrary.com.]

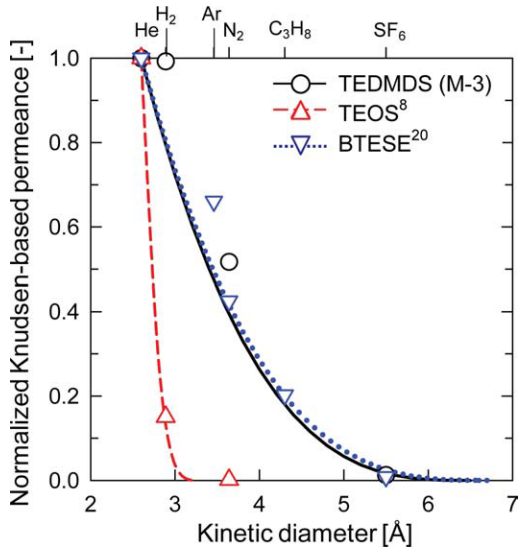

Figure 10. Normalized Knudsen-based permeance of TEDMDS (M-3), TEOS,[8] and BTESE[20]-derived silica membranes at 200°C are calculated as a function of kinetic diameter curves.

Normalized Knudsen-based permeance for TEDMDS (M-3), TEOS, and BTESE-derived silica membranes were calculated for d_p = 6.5, 3.2, and 6.8 Å, respectively, using Eq. 9. [Color figure can be viewed in the online issue, which is available at wileyonlinelibrary.com.]

Similar pore size distributions were observed despite the different calcination temperatures, probably due to the decomposition of methyl groups and resintering at high temperatures. An M-3 TEDMDS-derived membrane also showed a high H_2/SF_6 perm-selectivity of 660 and a low H_2/N_2 perm-selectivity (~10) with a high hydrogen permeance of 1.1×10^{-6} mol m^{-2} s^{-1} Pa^{-1}, and showed a pore size distribution similar to BTESE-derived silica membrane. On the other hand, a TEOS-derived silica membrane showed a high H_2/N_2 perm-selectivity of 1000 with a low hydrogen permeance. Interestingly, TEDMDS and BTESE-derived silica membranes showed higher H_2 permeance than He, while He permeance was higher than H_2 permeance for the TEOS-derived silica membrane. This suggests that the permeation of He is governed by Knudsen diffusion through the loose amorphous networks, confirming that TEDMDS and BTESE-derived silica membranes had a much looser structure than TEOS-derived silica membrane.

Normalized Knudsen-based permeance for TEDMDS (M-3), TEOS,[8] and BTESE-derived silica membranes[20] at 200°C as a function of kinetic diameter is shown in Figure 10. It should be noted that normalized Knudsen-based permeance (NKP) equals to unity under Knudsen diffusion mechanism, therefore, TEDMDS, TEOS, and BTESE-derived silica membranes showed NKPs smaller than one due to molecular sieving effect. Fitting curves were calculated using Eq. 9. Judging from fitting curves based on Eq. 9 for TEDMDS, TEOS, and BTESE-derived silica membranes, the order of pore size can be estimated as follows: TEOS-derived silica membrane <M-3 TEDMDS-derived silica membrane ≅ BTESE-derived silica membrane. BTESE and TEDMDS-derived silica membrane showed a larger pore size distribution than TEOS-derived silica membrane. This suggests that silica membranes created by a Si single unit alkoxide (TEOS) showed smaller pore size distribution than silica membranes prepared by a bridged alkoxide unit, such as Si—O—Si or Si—C—C—Si. It can be concluded that the membrane pore size or membrane structure can be tuned for larger pore sizes with TEDMDS-based Si—O—Si bonding.

Pore size tuning by in situ heat treatment

Siloxane compounds having organic groups such as methyl or phenyl were used for a template to create a continuous network of micropores by the removal of organic ligands embedded in a dense inorganic matrix.[9–18] The pyrolysis of organic groups in a membrane matrix showed the loose structure of the membrane network. Since the TEDMDS silica precursor consists of thermally stable —Si—O—Si— bonding as a main chain, and has two methyl groups that can be used as a template by pyrolysis in an air atmosphere, TEDMDS has an advantage in tuning pore size by the "template" (methyl group) and "spacer" (—Si—O—Si— bonding) techniques. M-4 membrane prepared at 550°C under a N_2 atmosphere, having few or no defects, was used for the investigation of pore size tuning by in situ heat treatment. Figure 11 shows the time course of air permeance for M-4 TEDMDS-derived silica membrane during exposure to air at 300, 450, and 550°C where the temperatures were increased under He flow after confirming a steady flow at each temperature. Air permeance for M-4 membrane during the exposure to air was constant at 300°C and increased slightly at 450°C, showing thermal stability at 300–450°C. However, air permeance drastically increased from 10^{-7} to 10^{-6} at 550°C, which was close to that of the intermediate layer, resulting in a broken membrane structure of the combustion of methyl group, as shown in Figure 7.

After confirming a steady-state of air permeance at each temperature, gas permeances at 200°C were measured to evaluate the pore size distribution. Figure 12 shows gas permeances of M-4 membrane at 200°C before (fresh membrane) and after exposure to air at 300 and 450°C. All gas permeances were similar before and after treatment at 300°C in air. On the other hand, H_2/N_2 and H_2/SF_6 perm-selectivity

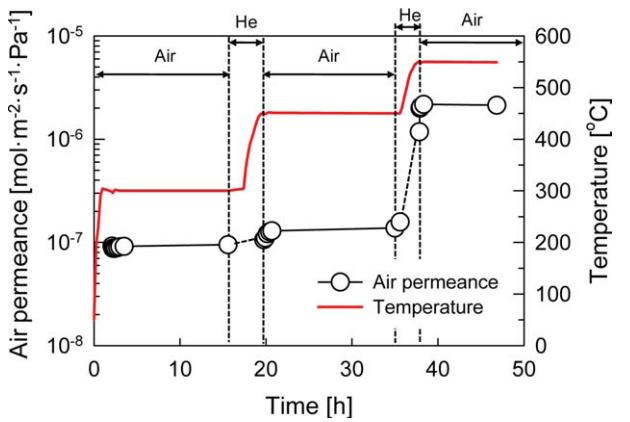

Figure 11. Time course of air permeance for TEDMDS-derived silica membrane (M-4) during exposure to air.

[Color figure can be viewed in the online issue, which is available at wileyonlinelibrary.com.]

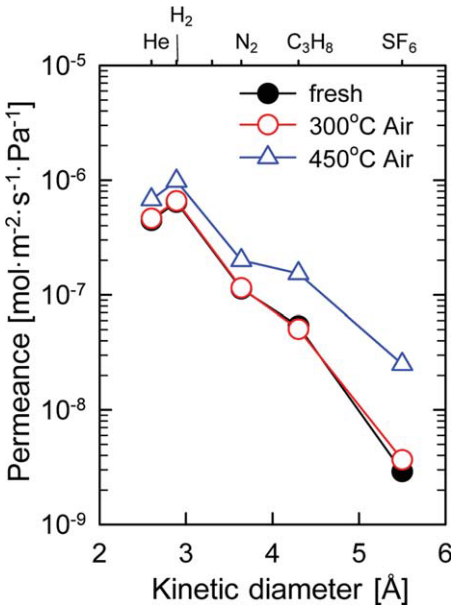

Figure 12. Gas permeance for TEDMDS-derived silica membrane (M-4) at 200°C before and after exposure to air at 300 and 450°C.

[Color figure can be viewed in the online issue, which is available at wileyonlinelibrary.com.]

for M-4 membrane treated in air at 450°C showed 4.9 and 39.3, respectively, and gas permeation increased compared with fresh membrane, suggesting that the pyrolysis of methyl groups in the membrane surface enlarged the pore size of the "template."

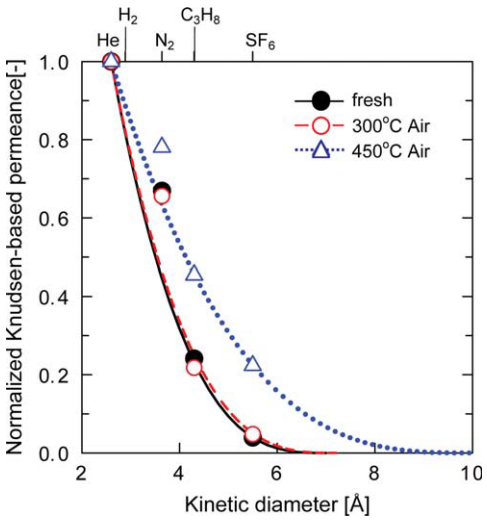

Figure 13. Normalized Knudsen-based permeance of TEDMDS-derived silica membranes at 200°C before and after exposure to air at 300 and 450°C as a function of kinetic diameter.

Normalized Knudsen-based permeance for fresh M-4 TEDMDS-derived membrane, and after exposure to 300 and 450°C in an air atmosphere, was calculated for d_p = 7.0, 7.2, and 10.0 Å, respectively, using Eq. 9. [Color figure can be viewed in the online issue, which is available at wileyonlinelibrary.com.]

Table 1. Perm-Selectivity of He/H_2 and Activation Energy at 200°C Before and After Exposure to Air at Each Temperature

		E_p [kJ mol^{-1}]	
	He/H_2	He	H_2
Fresh	0.70	5.62	2.63
300°C Air	0.70	5.71	1.94
450°C Air	0.69	2.90	1.10

Figure 13 shows the dimensionless permeance for M-4 membrane, fresh and after exposure to an air atmosphere at different temperatures. Judging from the fitting curve based on Eq. 9 for M-4 TEDMDS-derived silica membranes, the order of pore size can be calculated as follows: fresh M-4 membrane ≈M-4 membrane treated at 300°C in air <M-4 membrane treated at 450°C in air. Judging from normalized Knudsen-based permeance, the pores appeared to be enlarged ~3 Å, which possibly corresponds to the size of the methyl groups. These results suggest that the pore size of TEDMDS-derived silica membrane can be tuned by different temperatures and gas atmospheres.

Table 1 shows the perm-selectivity of He/H_2 at 200°C and activation energy before and after exposure to air at each temperature. The activation energy obtained by Eq. 4 for M-4 membrane after exposure to air at 450°C decreased from 5.62 to 2.90 kJ mol^{-1} for He permeation and 2.63 to 1.10 kJ mol^{-1}

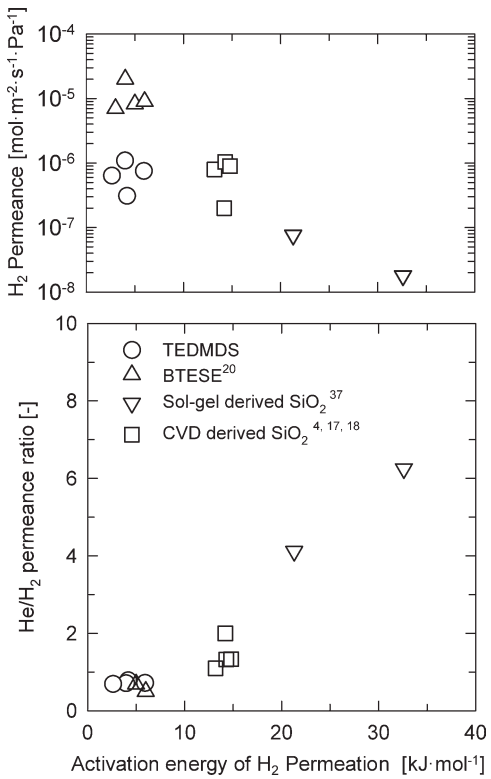

Figure 14. He/H_2 permeance ratio as a function of activation energy of H_2 permeation at 200°C for TEDMDS-derived silica membranes (M-1 to M-4), Sol-gel[37] (after hydrothermal treatment) and CVD derived silica membranes,[4,17,18] and BTESE-derived silica membranes.[20]

for H_2 permeation, respectively. Hecarlioglu et al.[36] reported activation energy for the permeation of He and H_2 through silica membranes in an ab initio calculation study. They clearly showed that activation energy increased with a decrease in silica members rings, which corresponded to pore sizes. The activation energy of TEDMDS-derived silica membrane also decreased as firing temperature increased, which is consistent with membrane pore size as shown in Figure 13.

Figure 14 shows the He/H_2 permeance ratio as a function of the activation energy of H_2 permeance at 200°C for TEDMDS-derived silica membranes, sol-gel[37] and CVD derived silica membranes,[4,17,18] and BTESE-derived silica membranes.[20] The He/H_2 permeance ratio increased with increasing activation energy of H_2 permeation. This is because a He/H_2 permeance ratio can be considered a measure of pore size distribution of silica where He and H_2 can permeate.[20] Silica membranes prepared by sol-gel and CVD showed activation energies in the range of 10–40 kJ mol^{-1}. On the other hand, the activation energy of BTESE and TEDMDS-derived silica membrane was in the range of 1–10 kJ mol^{-1}. Judging from the activation energy, the structure of the TEDMDS and BTESE-derived silica membrane is more open, due to —Si—O—Si— and Si—C—C—Si, than that of silica membrane prepared by the sol-gel and CVD method. The upper part of Figure 14 shows H_2 permeance for TEDMDS-derived silica membrane, silica membranes by sol-gel and CVD, and BTESE-derived silica membranes. Although both TEDMDS and BTESE-derived silica membranes showed an activation energy in the range of 1–10 kJ mol^{-1}, the H_2 permeance of BTESE-derived silica membrane was one order higher than that of TEDMDS-derived silica membrane. The reason is not yet clear, but one possible reason might be the existence of a methyl group in the case of TEDMDS. The methyl group in the silica networks might exert a strong influence on hydrogen permeation through TEDMDS-derived silica membranes, or reduce the effective pore area for the permeation of gases.

Conclusions

Normalized Knudsen-based permeance was proposed for pore size determination. TEDMDS-derived silica membranes to control the amorphous structure were prepared with TEDMDS by the sol-gel technique at different firing temperatures.

(1) A normalized Knudsen-based permeance, which was derived from the GT permeation model with proper assumptions, was proposed as a convenient and easy-to measure technique to evaluate the pore sizes of microporous membranes, and verified using the permeance of zeolite membranes.

(2) Crack-free TEDMDS-derived silica membranes (membrane thickness: 200 nm) showed high H_2 permeance (0.3–1.1 $\times$ 10^{-6} mol m^{-2} s^{-1} Pa^{-1}) with low H_2/N_2 ($\sim$10) and high H_2/SF_6 ($\sim$1200) perm-selectivity compared with TEOS-derived silica membrane at 200°C. Pore size distribution, determined by single gas permeation, suggested TEDMDS-derived silica membrane had loose amorphous silica structure due to the existence Si—O—Si as a "spacer."

(3) TEDMDS-derived silica membrane prepared at 550°C in an N_2 atmosphere showed thermal stability before and after exposure to air at 300°C, while gas permeance increased with low perm-selectivity during air exposure between 450 and 550°C. The pyrolysis of methyl groups in the membrane surface enlarged membrane pore size as a "template" technique, presenting the possibility of membrane pore size tuning with organic ligands by changes in the calcination temperature.

(4) TEDMDS-derived silica membranes showed a good correlation between the He/H_2 permeance ratio and the activation energy of H_2 permeation. The activation energies of TEDMDS-derived silica membrane were in the range of 3–6 kJ mol^{-1}.

Notation

P_K = permeance in the Knudsen mechanism, mol m^{-2} s^{-1} Pa^{-1}
d_p = pore radius, m
L = membrane thickness, m
M = molecular weight, g mol^{-1}
T = temperature, K
R = gas constant, J mol^{-1} K^{-1}
E_p = kinetic energy, J mol^{-1}
A_i = area of the pore opening for effective for permeation of i-th component, m^2
A_o = cross-sectional area of the pore, m^2
f = normalized Knudsen-based permeance
$d_{k,i}$ = molecular size of i-th component, m

Greek letters

ε = membrane porosity
τ = tortuosity
ρ = probability
$\rho_{g,i}$ = probability of i-th component

Literature Cited

1. Verweij H, Lin JYS, Dong J. Microporous silica and zeolite membranes for hydrogen purification. *MRS Bull*. 2006;31:1–10.
2. Dong J, Lin YS, Kanezashi M, Tang Z. Microporous inorganic membranes for high temperature hydrogen purification. *J Appl Phys*. 2008;104:121301–121317.
3. Kim SS, Sea BK. Gas permeation characteristics of silica/alumina composite membrane prepared by chemical vapor deposition. *Korean J Chem Eng*. 2001;18:322–329.
4. Gu Y, Hacarlioglu P, Oyama ST. Hydrothermally stable silica-alumina composite membranes for hydrogen separation. *J Membr Sci*. 2008;310:28–37.
5. Gopalakrishnan S, Yoshino Y, Nomura M, Nair BN, Nakao S. A hybrid processing method for high performance hydrogen-selective silica membranes. *J Membr Sci*. 2007;297:5–9.
6. Gopalakrishnan S, Diniz da Costa JC. Hydrogen gas mixture separation by CVD silica membrane. *J Membr Sci*. 2008;323:144–147.
7. de Vos RM, Verweij H. Improved performance of silica membranes for gas separation. *J Membr Sci*. 1998;143:37–51.
8. Tsuru T. Nano/subnano-tuning of porous ceramic membranes for molecular separation. *J Sol-Gel Sci Technol*. 2008;46:349–361.
9. Raman NK, Brinker CJ. Organic "template" approach to molecular sieving silica membranes. *J Membr Sci*. 1995;105:273–279.
10. Duke MC, Diniz da Costa JC, Lu Max GQ, Petch M, Gray P. Carbonised template molecular sieve silica membranes in fuel processing systems: permeation, hydrostability and regeneration. *J Membr Sci*. 2004;241;325–333.
11. Duke MC, Diniz da Costa JC, Do DD, Gray PG, Lu GQ. Hydrothermally robust molecular sieve silica for wet gas separation. *Adv Funct Mater*. 2006;16:1215–1220.
12. Moon JH, Park YJ, Kim MB, Hyun SH, Lee CH. Permeation and separation of a carbon dioxide/nitrogen mixture in a methyltriethoxysilane templating silica/α-alumina composite membrane. *J Membr Sci*. 2005;250:195–205.

13. Kusakabe K, Sakamoto S, Saie T, Morooka S. Pore structure of silica membranes formed by a sol-gel technique using tetraethoxysilane and alkyltriethoxysilane. *Sep Purif Technol*. 1999;16:139–146.
14. Kim YS, Kusakabe K, Morooka S, Yang SM. Preparation of microporous silica membranes for gas separation. *Korean J Chem Eng*. 2001;18:106–112.
15. Sea BK, Watanabe M, Kusakabe K, Morooka S, Kim SS. Formation of hydrogen permselectivity silica membrane for elevated temperature hydrogen recovery from a mixture containing steam. *Gas Sep Purif*. 1996;10:187–195.
16. Sea BK, Kusakabe K, Morooka S. Pore size control and gas permeation kinetics of silica membranes by pyrolysis of phenyl-substituted ethoxysilanes with cross-flow through a porous support wall. *J Membr Sci*. 1997;130:41–52.
17. Ohta Y, Akamatsu K, Sugawara T, Nakao A, Miyoshi A, Nakao S. Development of pore size-controlled silica membranes for gas separation by chemical vapor deposition. *J Membr Sci*. 2008;315:93–99.
18. Nomura M, Nagayo T, Monma K. Pore size control of a molecular sieve silica membrane prepared by a counter diffusion CVD method. *J Chem Eng Jpn*. 2007;40:1235–1241.
19. Kanezashi M, Yada K, Yoshioka T, Tsuru T. Design of silica networks for development of highly permeable hydrogen separation membranes with hydrothermal stability. *J Am Chem Soc*. 2009;131:414–415.
20. Kanezashi M, Yada K, Yoshioka T, Tsuru T. Organic-inorganic hybrid silica membranes with controlled silica network size: Preparation and gas permeation characteristics. *J Membr Sci*. 2010;348:310–318.
21. Tsuru T, Takata Y, Kondo H, Hirano F, Yoshioka T, Asaeda M. Characterization of sol-gel derived membranes and zeolite membranes by nanopermporometry. *Sep Purif Technol*. 2003;32:23–27.
22. Duke MC, Pas SJ, Hill AJ, Lin YS, da Costa JC. Exposing the molecular sieving architecture of amorphous silica using positron annihilation spectroscopy. *Adv Funct Mater*. 2008;18:3818–3826.
23. Xiao J, Wei J. Diffusion mechanism of hydrocarbons in zeolites—I. Theory. *Chem Eng Sci*. 1992;47:1123–1141.
24. Shelekhin AB, Dixon AG, Ma YH. Theory of gas diffusion and permeation in inorganic molecular-sieve membranes. *AIChE J*. 1995;41:58–67.
25. Yoshioka T, Nakanishi E, Tsuru T, Asaeda M. Experimental study of gas permeation through microporous silica membranes. *AIChE J*. 2001;47:2052–2063.
26. Baker RW. *Membrane Technology and Applications*, *2nd ed*. Chichester: Wiley. 2004.
27. Lee HR, Kanezashi M, Yoshioka T, Tsuru T. Preparation of hydrogen separation membranes using disiloxane compounds. *Desal Water Treat*. 2010;17:120–126.
28. Kanezashi M, Lin YS. Gas permeation and diffusion characteristics of MFI-type zeolite membranes at high temperatures. *J Phys Chem C*. 2009;113:3767–3774.
29. Kanezashi M, O'Brien-Abraham J, Lin YS. Gas permeation through DDR-type zeolite membranes at high temperature. *AIChE J*. 2008;54:1478–1486.
30. Lovallo MC, Gouzinis A, Tsapatsis M. Synthesis and characterization of oriented MFI membranes prepared by secondary growth. *AIChE J*. 1998;44:1903–1913.
31. Lindmark J, Hedlund J. Modification of MFI membranes with amine groups for enhanced CO_2 selectivity. *J Mater Chem*. 2010;20:2219–2225.
32. van den Bergh J, Zhu W, Kapteijn F, Moulijn J, Yajima K, Nakayama K, Tomita T, Yoshida S. Separation of CO_2 and CH_4 by a DDR membrane. *Res Chem Intermed*. 2008;34:467–474.
33. van den Bergh J, Tihaya A, Kapteijn F. High temperature permeation and separation characteristics of an all-silica DDR zeolite membrane. *Microporous Mesoporous Mater*. 2010;132:137–147.
34. de Vos RM, Maier WF, Verweij H. Hydrophobic silica membranes for gas separation. *J Membr Sci*. 1999;158:277–288.
35. Innocenzi P, Abdirashid MO, Guglielmi M. Structure and properties of sol-gel coatings from methyltriethoxysilane and tetraethoxysilane. *J Sol-Gel Sci Technol*. 1994;3:47–55.
36. Hacarlioglu P, Lee D, Gibbs GV, Oyama ST. Activation energies for permeation of He and H_2 through silica membranes: an ab initio calculation study. *J Membr Sci*. 2008;313:277–283.
37. Kanezashi M, Asaeda M. Stability of H_2-permselective Ni-doped silica membranes in steam at high temperature. *J Chem Eng Jpn*. 2005;38:908–912.

Manuscript received June 23, 2010, and revision received Oct. 28, 2010.